Applied Nanoscience (2020) 10:3411–3420
https://doi.org/10.1007/s13204-020-01469-w

ORIGINAL ARTICLE

Development of gold nanoclusters based direct fluorescence restoration approach for sensitive and selective detection of pesticide

Kanwal Nazir[1] · Ayesha Ahmed[1] · Syed Zajif Hussain[2] · Muhammad Rizwan Younis[3] · Yumna Zaheer[1] · Mukhtair Ahmed[4] · Irshad Hussain[2] · Ayesha Ihsan[1]

Received: 12 February 2020 / Accepted: 28 May 2020 / Published online: 29 June 2020

Abstract

Pesticide contamination of drinking water is of high concern due to their hazardous effects on ecosystems. Several detection methods are available which are associated with many drawbacks, e.g. slow response time and laborious procedural techniques. This limits their practicability. Therefore, there is a dire need to develop quick, simpler but equally sensitive and practical methods for pesticide detection. Herein, we report a highly sensitive assay using fluorescent AuNCs for the detection of a pesticide i.e., 2-methyl-4-chlorophenoxyacetic acid (MCPA). For this purpose, three different fluorescent Au nanoclusters stabilized by histidine (His-AuNCs), lysozyme (Lys-AuNCs) and RNase (RNase-AuNCs) were systematically studied as optical probes for the detection of MCPA using a turn-on assay. The fluorescence of these AuNCs was initially quenched with Cu^{2+} ions followed by the quantitative recovery of their fluorescent signals in the presence of MCPA. The sensitivity and selectivity of these clusters for MCPA were in a linear dynamic range, i.e., 110–180 nM, 100–170 nM and 90–160 nM in case of His-AuNCs, Lys-AuNCs and RNase-AuNCs, respectively. Also, the aforesaid clusters were having a different limit of detection (LOD) by each type, i.e., highest by His-AuNCs (21.87), intermediate by Lys-AuNCs (12.97) and lowest by RNase-AuNCs (9.26 nM). Hence, the RNase-AuNCs are found to be the most sensitive, whereas His-AuNCs are least sensitive for the detection of MCPA. These findings offer a rapid, sensitive and selective assay for MCPA detection and have potential implications for the on-site, real-time monitoring of noxious pollutants.

Keywords Fluorescence restoration · Quenching · Gold nanoclusters · Fluorescent sensing · Pesticide · 2-Methyl-4-chlorophenoxyacetic acid

Introduction

Pesticides are one of the several ubiquitous classes of organic compounds, which have widely been used by farmers to eliminate the threat of common pests and to increase the yield of crops. However, their use has been of serious concern due to their unwanted persistence in the environment and suspected toxicity to the aquatic and terrestrial life (Zhao 2017). Among various classes of pesticides, organochlorine pesticides (OCPs) have always been of serious concern in this context (Eto 2018). In spite of their effective pest-control role, OCPs are known for their unusual long residual action and persistence in the environment without losing their toxicity (Carvalho 2017). These factors favor their environmental bio-accumulation, causing long-term damage to both terrestrial and aquatic life (Katagi 2010). Among all the OCPs, phenoxyacetic herbicides are the most widely used to eliminate broadleaf weeds. Due to

Electronic supplementary material The online version of this article (https://doi.org/10.1007/s13204-020-01469-w) contains supplementary material, which is available to authorized users.

✉ Ayesha Ihsan
aishaehsan@nibge.com

[1] National Institute for Biotechnology and Genetic Engineering, Jhang Road, Faisalabad, Pakistan

[2] Department of Chemistry and Chemical Engineering, SBA School of Science and Engineering (SSE), Lahore University of Management Sciences (LUMS), DHA, Lahore 54792, Pakistan

[3] Marshall Laboratory of Biomedical Engineering, International Cancer Center, Laboratory of Evolutionary Theranostics (LET), School of Biomedical Engineering, Shenzhen, University Health Science Center, Shenzhen 518060, China

[4] Department of Chemistry, Quaid-I-Azam University, Islamabad 45320, Pakistan

their selective effect on broadleaf weeds, this subclass is highly preferred to protect grain crops throughout the world (Skiba et al. 1987). This group of pesticides and its metabolites have been found to have adverse health effects such as cancer, neurological damage, birth deformities and damage to the human nervous system (Damalas and Eleftherohorinos 2011). Generally, the use of pesticides is comparatively higher in South Asian and African countries such as Pakistan, India, Bangladesh, and Algeria. This is due to the climatic conditions as high temperature and humidity are very favorable for the pest growth (Jayaraj et al. 2016). In general, an upsurge of ~ 25% per year is observed for such pesticides in Pakistan (Kalwar et al. (2015)). There is, therefore, a dire need to develop a simple, efficient but equally economical protocols for the monitoring and quantification of such compounds to cater for the environmental security and food hygiene.

Despite their high sensitivity, conventional detection approaches such as chromatographic (Dias 2015), electrochemical (Anirudhan and Alexander 2015) and enzyme-linked immunosorbent assays (ELISA) (Heys 2017) are not considered much feasible due to the associated complicities, tedious sample preparation steps and uneconomic nature (Kumar et al. 2015). Conversely, the fluorescent detection methods are known for their simplicity, easy approach, and cost-effective nature. The key feature of the fluorescent methods is their rapid response time as compared to all other related analytical techniques. In this regard, a number of smart fluorescent materials have been reported to detect various contaminants (Kumar et al. 2015; Gao et al. 2017). However, the choice of fluorescent materials is highly influenced by the nature of analyte under investigation. In addition, despite all other merits of fluorescent methods, these methods are not as sensitive as other sophisticated techniques such as HPLC and spectrometry. Therefore, the exploration of more sensitive fluorescent materials, with the capability to transform minute detection of chemical changes into robust fluorescent signals, is highly desired. The use of fluorescent dyes (Walton 2012; Markechová et al. 2013) and quantum dots (Li 2018) has been reported as a promising approach, but the associated photo-bleaching problems (Wang et al. 2015; Zheng 2014) and toxic nature of heavy-metal-based quantum dots (Wang 2013; Tsoi 2013) limit the widely-accepted applications of such probing agents.

Metal nanoclusters (MNCs) have promising optical characteristics based on their ultra-small size, good biocompatibility and tunable bright fluorescence (Goswami 2016; Li et al. 2014). These MNCs have been used for the sensitive and selective detection of various analytes and are now considered suitable alternatives to the conventional probing agents. Among the common MNCs, gold nanoclusters (AuNCs) are very interesting due to their embellished characteristics compared to other competitors (Lu et al. 2017; Lin 2009). The gold core of the clusters is usually stabilized in solution by the ligand shell e.g. proteins, polymers, DNA and even small molecules. This ligand shell-metal core structure of gold nanoclusters endows them more stability and sensitivity as both metalcore and ligand shell interact with the target compounds to increase the overall reaction sensitivity. The AuNCs have been signified for the sensitive detection of neurotransmitters (Zhang, et al. (2017)), enzymes (Luo 2016), urea (Deng 2016), glucose (Lai 2017), drugs (Jiang et al. 2016), biomarkers (Ramesh 2016) and reactive oxygen species (Zhou et al. 2016). Nonetheless, their applications for effective detection of pesticide is still quite less-explored. Very recently, Su et al., reported an electrochemical pesticide detection method using tyrosinase enzyme quenched fluorescence of gold nanoclusters stabilized on the egg membrane (Yan 2017). The authors indirectly determined the organophosphate pesticide by first inhibiting the fluorescence of AuNCs by dopaminechrome, an oxidation product of tyrosinase. Upon the addition of organophosphate, the fluorescence of gold nanoclusters was restored. The method is sensitive enough but it is a bit complicated and involves expensive reagents. To the best of our knowledge, there is no direct assay available for the detection of OCs while using MNCs. Herein, we report a direct fluorescence restoration approach for the sensitive and selective detection of an organochlorine pesticide i.e., 2-methyl-4-chlorophenoxyacetic acid (MCPA). In addition to presenting the first report on gold nanoclusters based direct assay for pesticide detection, the unique point of this study is that the findings of this assay were validated using three different types of fluorescent probes i.e., histidine coated AuNCs (His-AuNCs), lysozyme coated gold nanoclusters (Lys-AuNCs) and RNase coated gold nanoclusters (RNase-AuNCs). The corresponding fluorescence signals of all these nanoprobes were quenched in the presence of Cu^{2+} ions and fluorescence restoration was achieved with the addition of MCPA. The fluorescence restoration, caused by the relatively high affinity between Cu^{2+} and the carboxyl group of MCPA, led to the sensor development with linear dynamic range and sensitivity reaching down to ~ 90 nM for MCPA (using RNase-AuNCs). The concentration of MCPA was quantified according to the respective shift in fluorescence intensity, and the obtained results were validated by calculating *Rr* (restoration constant) via concentration-dependent restoration curves for MCPA detection, determined separately for each type of fluorescent nanoclusters.

Experimental

Reagents

Hydrogen tetrachloroaurate (III) hydrate ($HAuCl_4 \bullet 4H_2O$), lysozyme, ribonuclease (RNase), histidine, MCPA, chloride salts of metals including; Na^+, K^+, Mg^{2+}, Ca^{2+}, Ba^{2+}, Co^{2+},

Ni^{2+}, Zn^{2+}, Mn^{2+}, Cu^{2+}, Cd^{2+}, Al^{3+}, Cr^{3+} and Pb^{2+} were of all analytical grade and purchased from Sigma Aldrich. Milli-Q water produced by Millipore water purification system (18.2 MΩ cm^{-1}) was used throughout this work.

Instrumentation

The hand-held UV lamp was purchased from Herolab. UV–Vis and Nanoseries Zetasizer (Malvern Instruments) was used for the determination of surface charge of the clusters. Alpha FTIR was purchased from Bruker Corporation. Heto PowerDry LL 1500 Freeze Dryer was acquired from Thermo Electron Corporation. 2300-001 M EnSpire® Multimode Plate Reader was purchased from Perkin Elmer. Shaking incubator was procured from Kuhner Instruments. All the glassware was oven (Fisher Scientific) dried before use. For homogenizing the solutions, a sonicator obtained from Elma was used. pH measurements were performed using a pH meter (InoLab).

Synthesis of gold nanoclusters

Histidine protected AuNCs were prepared as per the previously reported method (Yang 2011). Briefly, 1 mL of 0.01 M aqueous solution of $HAuCl_4$ was added to 3 mL aqueous solution of 0.5 M histidine and incubated (37 °C) for about 30 h. The lysozyme-stabilized AuNCs (Lys-AuNCs) were also synthesized according to a previously reported method with slight modification (Chen et al. 2010). For this purpose, 2 mL of 5 mM aqueous $HAuCl_4$ solution was added to 32.4 mg/mL aqueous solution of lysozyme followed by the addition of 160 µL of 1 M sodium hydroxide solution. The mixture was incubated at 37 °C for about 30 h. The RNase-coated AuNCs were also prepared using the previously reported procedure (Kong 2013), and the optimized recipe in this regard was obtained. Briefly, 1 mL of $HAuCl_4$ (5 mM aqueous solution) was added to 100 mg/mL aqueous solution of RNase-A. Then 100 µL of 1 M sodium hydroxide solution was added to the mixture and incubated at 37 °C for ~ 30 h. After the completion of approximate incubation, the fluorescence of all nanoclusters was examined under UV light at an excitation wavelength of 365 nm. Red fluorescence was observed for lysozyme and RNase-coated AuNCs whereas a bluish-green fluorescence was observed for His-AuNCs. RNase-AuNCs and Lys-AuNCs were dialyzed against ultrapure water for 24 h using a 20 kDa dialysis membrane for purification whereas His-AuNCs were purified using syringe filtration (0.45 µm) owing to the smaller size of the capping amino acid, i.e., histidine (155.15 g/mol) (Yang 2011). After purification, the fluorescence intensity increased by 9%, 8.9% and 7.8% in the case of RNase-AuNCs, Lys-AuNCs and His-AuNCs, respectively (Fig. S-1 A, B, C). Purified AuNCs were then concentrated by freeze-drying under vacuum. All the fluorescence studies were performed using a multimode plate reader while placing the samples in a 96-well microplate.

Fluorescence quantum yield calculation

For RNase and Lys-AuNCs, the quantum yield was calculated using Fluorescein isothiocyanate (FITC) as a reference with a standard quantum yield of 92%. For His-AuNCs, tryptophan was used as a reference with a standard quantum yield of 20% (Fig. S-2 A, B). For spectral measurements, reference and AuNCs were diluted with deionized water to yield an absorbance of ~ 0.1 at 480 nm and following equation (Ibrahim et al. 2017) was used for the calculation:

$$\emptyset_X = \emptyset_R \frac{Grad_x}{Grad_R} \frac{\eta_X^2}{\eta_R^2},$$

where $\emptyset_R$ = Quantum yield of the reference, $\emptyset_X$ = Quantum yield of the analyte, $Grad_R$ = Gradient from the plot of integrated fluorescence intensity vs absorbance of the reference, $Grad_X$ = Gradient from the plot of integrated fluorescence intensity vs absorbance of the analyte, η_R = Refractive index of the reference, η_X = Refractive index of the analyte.

Fluorescence turn-on studies for MCPA detection

The fluorescence restoration experiments were carried out using a series of dilutions of MCPA. The fluorescence of the AuNCs was first quenched by Cu^{2+} ions, which was subsequently restored by adding MCPA. The AuNCs were tested for various operational parameters followed by interference studies for other pesticides such as malathion, 2,4-dichlorophenoxyacetic acid (2,4-D) and metribuzin as well as anionic species such as Br^{1-}, I^{1-}, Cl^{1-}, F^{1-}, OH^{1-}, NO_3^{1-} and PO_4^{3-}. The limit of detection for the fluorescence restoration was determined for each of the three types of AuNCs.

Data analysis

To determine and interpret the relationship between the fluorescence restoration and comparative sensitivity of the AuNCs, a restoration equation was used ($Rr = ((F_o/F[Q]) - 1)/[Q]$) and a linear correlation model was developed by plotting the ratio of F_o and F against the respective concentrations of MCPA added to each type of AuNCs. The values of dF ($F_0 - F$) were calculated as a response function to evaluate the fluorescence restoration. The Rr (restoration constant) values for all the nanoclusters were calculated from the slope of the linear correlation plot. Moreover, the linear regression correlation coefficient was also determined to examine the significance of correlation parameters. Limit of detection (LOD), limit of quantification (LOQ) and signal

to noise S/N values were also determined for each type of cluster.

Results and discussion

All nanoclusters i.e. His-AuNCs Lys-AuNCs and RNase Au-NCs were synthesized as per previously reported methods, their quantum yields were calculated separately, which were found to be ~ 18% for RNase-AuNCs, ~ 12% for Lys-AuNCs and ~ 6% for His-AuNCs (Fig. S-3 A, B & C) and is in accordance with the literature (Li et al. 2014; Yang 2011; Chen et al. 2010; Shamsipur 2015). Quantum yield of nanoclusters is usually dependent on the ligand–metal core interaction. RNase is a smaller protein (13.7 kDa), which may facilitate efficient penetration of gold ions to interact with the functional group of proteins (Kong 2013). The protein gold interaction can be observed by the FTIR scan of both RNase-AuNCs and Lys-AuNCs.

In both cases (RNase and Lys-AuNCs), the gold surface is not much saturated with Au–S bonds (Yan 2017). Gold ions might have bound to amino groups in the protein. This supposition can be proved by FTIR studies (Fig. 1a–c) where a redshift in amide I (mainly C=O stretching) and amide II (N–H bending coupled with C–N stretching) bands can be assigned to Au–N bond.

It suggests that most of the electron density on the surface of clusters is due to the protein functional groups other than Au–S bond (Guével 2011). Lysozyme protein has a comparatively larger size (14.3 kDa), which may limit the number of gold ions to interact with the functional groups of proteins. This may be the limiting factor for the efficient interaction of gold with protein core which may result in a relatively less quantum yield (Chen, et al. 2010). These may be the contributing factors for the relatively higher quantum yield of RNase-AuNCs as compared to that of Lys-AuNCs. FTIR spectrum of His-AuNCs shows the bonding of Au clusters with imidazole ring, which is evident by a red shift in N–H bending and C–N stretching (Shamsipur 2015). The absorbance behavior of all three AuNCs can be observed by their UV–visible spectra (Fig. 1d).

The characteristic protein absorbance peak at 280 nm due to tryptophan residue is visible in the absorption spectra of both Lysozyme and RNase clusters but missing in His-AuNCs. Moreover, the characteristic SPR band for gold nanoparticles is absent (500–600 nm), which shows

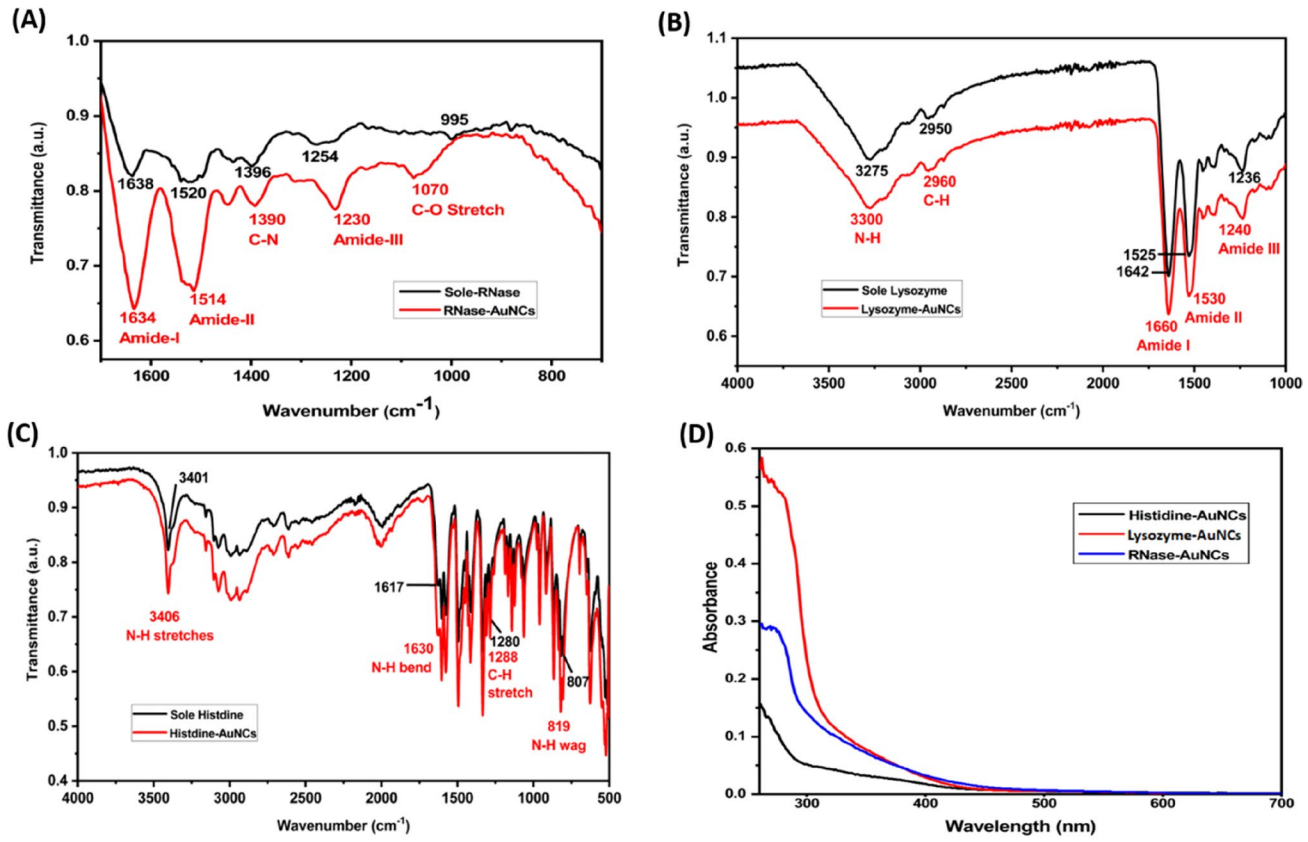

Fig. 1 FTIR spectra of RNase and RNase-AuNCs (**a**), Lysozyme and Lysozyme-AuNCs (**b**), and Histidine and Histidine-AuNCs (**c**), UV–Visible spectra of Histidine-AuNCs, Lysozyme-AuNCs and RNase-AuNCs (**d**)

the absence of nanoparticles (> 2 nm) and the presence of smaller gold nanoclusters. When excited at 365 nm, His-AuNCs exhibited bluish-green fluorescence having maximum emission at 483 nm (Fig. S-3 A), whereas, AuNCs coated with Lysozyme and RNase showed red fluorescence with a maximum emission at 643 nm and 647 nm, respectively (Fig. S-4 B & C).

Colloidal stability of each cluster was determined by recording the Zeta potential of each type of AuNCs (Fig. S-5 A, B & C), which was found to be − 43 mV, − 36 mV and − 33 mV for RNase-AuNCs, Lys-AuNCs and His-AuNCs respectively showing excellent colloidal stability all these Au NCs (Abtahi et al. 2018).

Taking advantage of fluorescence and the high quantum yield of these AuNCs, we set out to develop a direct fluorescent assay for MCPA detection. In this regard, we evaluated the fluorescence quenching of all these AuNCs initially. It is well-known that the paramagnetic ions such as Fe^{2+} and Cu^{2+} have a strong affinity to quench the fluorescence of different probes by intersystem crossing (ISC) (Oh 2016). This quenching may be due to the interaction of quencher species with the surrounding protein shell or any other functional groups residing over the AuNCs. The quenching effect has a robust relation with the concentration of quencher. In this work, copper ions were used as a potential fluorescence quencher (Tao 2015). It is interesting to note that the quenched fluorescence can be restored by adding some competitive analyte. A possible scheme of fluorescence quenching of MNCs with copper ions and restoration with MCPA is demonstrated in Fig. 2.

After adding 10 µM of copper, significant aggregation of proteins protected AuNCs was observed, which is attributed to the Cu^{2+} interaction with proteins or histidine shells on AuNCs. A concentration of ~ 1.5 µM of Cu^{2+} ions was used to quench the fluorescence intensity. The quenched fluorescence intensity was gradually restored by adding MCPA. This restoration is due to the affinity of the carboxyl group ($-COO^-$) present in MCPA to the Cu^{2+} ions (Fig. 3). The carboxyl group of MCPA is thought to be responsible for its long retention time in soil (Kah et al. 2007; Davies and Jabeen 2002). The interaction of Cu^{2+} with COO^- group present in many drugs has also been used to demonstrate AuNCs based fluorescence restoration assays (Chen 2012). We also validated the detection of copper ions as a fluorescence quencher using these three clusters. Copper is an important analyte that has a certain biological and environmental impact. Copper ions can react with molecular oxygen to form reactive oxygen species (ROS), which have the potential to damage proteins, nucleic acid and lipids, which may lead to certain neurodegenerative disorders and organ dysfunction. Its detection in water is also of high importance due to its toxic nature (Durgadas et al. 2011). The respective

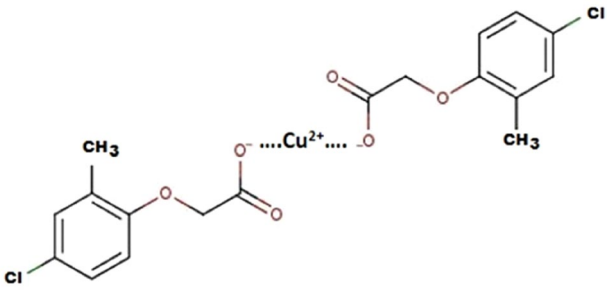

Fig. 3 The schematic illustration of the interaction between MCPA and copper

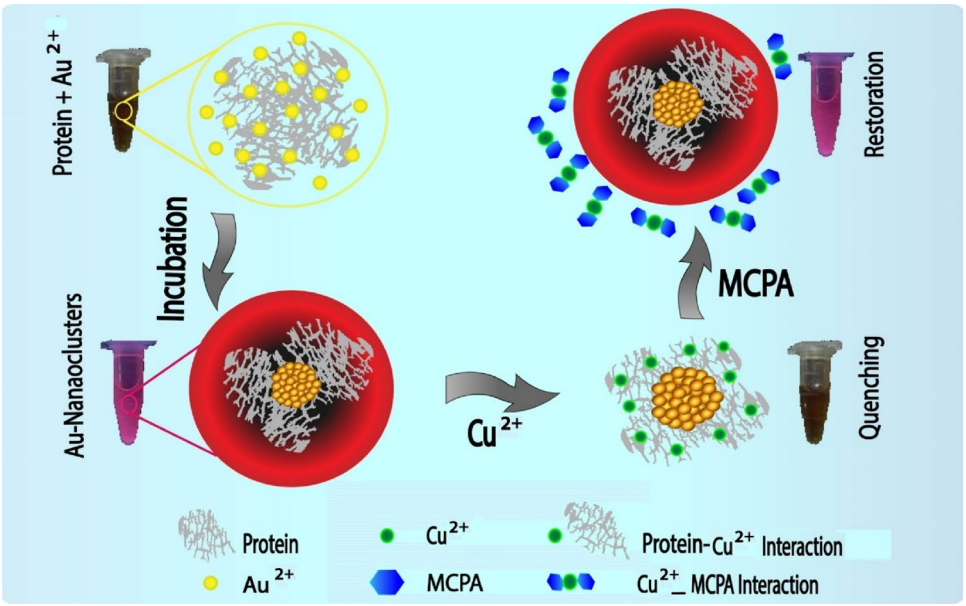

Fig. 2 The quenching and restoration scheme of fluorescent clusters against copper ions and pesticide molecules, respectively

results are given in the supporting information (Fig. S-6, A–F).

By gradual addition of MCPA, we observed a gradual restoration of fluorescence in all three types of AuNCs. This fluorescence restoration was found to be linearly dependent on the concentration of MCPA (Fig. 4). The reversible change of fluorescence suggested the stronger interaction of Cu^{2+} with carboxylic groups of MCPA. There was, however, no effect on the fluorescence of all three types of clusters by the direct addition of MCPA. Nevertheless, MCPA induced the aggregation of AuNCs at a higher concentration i.e., 5 µM, due to the protein hydrolyzing effect of MCPA. All these clusters exhibited an excellent response for the detection of MCPA, showing a linear correlation between the expression F/F_o and the concentration of MCPA (Fig. 4d–f).

RNase-AuNCs were, however, found to be the most sensitive with a fluorescence restoration response at even 90 nM of MCPA ($R^2 = 0.992$), while, Lys-AuNCs showed restoration response at 100 nM ($R^2 = 0.995$) and His-AuNCs were found to be least sensitive, as this probe started to show response at 110 nM with R^2 value of 0.985.

Fluorescence restoration LODs and LOQs were calculated via linear regression model for each type of AuNCs (Table 1), wherein 'σ' is the standard deviation and 'S' is the slope of linear regression curve. Moreover, background noise and signal to noise ratio had also been assessed and the estimated values tend to validate the data trend presented here.

To justify the sensitivity order of these probes, we first have to look at their binding affinity for copper ions because MCPA is detected due to its binding with copper ions. According to the suggested mechanism, Cu^{2+} ions are known to have high affinity with the histidine and other electron-rich species (such as $–NH_2$ and –COOH) on the protein surface (Durgadas et al. 2011). Due to the varying

Table 1 LODs and LOQs for His-AuNCs, Lys-AuNCs and RNase-AuNCs based on their respective linear regression model

AuNCs	LOD = 3σ/S (nM)	LOQ = 10σ/S (nM)	$Noise_{RMS}$	Signal/noise
His-AuNCs	21.87	72.89	10.15	31.03
Lys-AuNCs	12.97	43.23	7.7	69.48
RNase-AuNCs	9.26	30.86	6.65	91.72

RMS root mean square

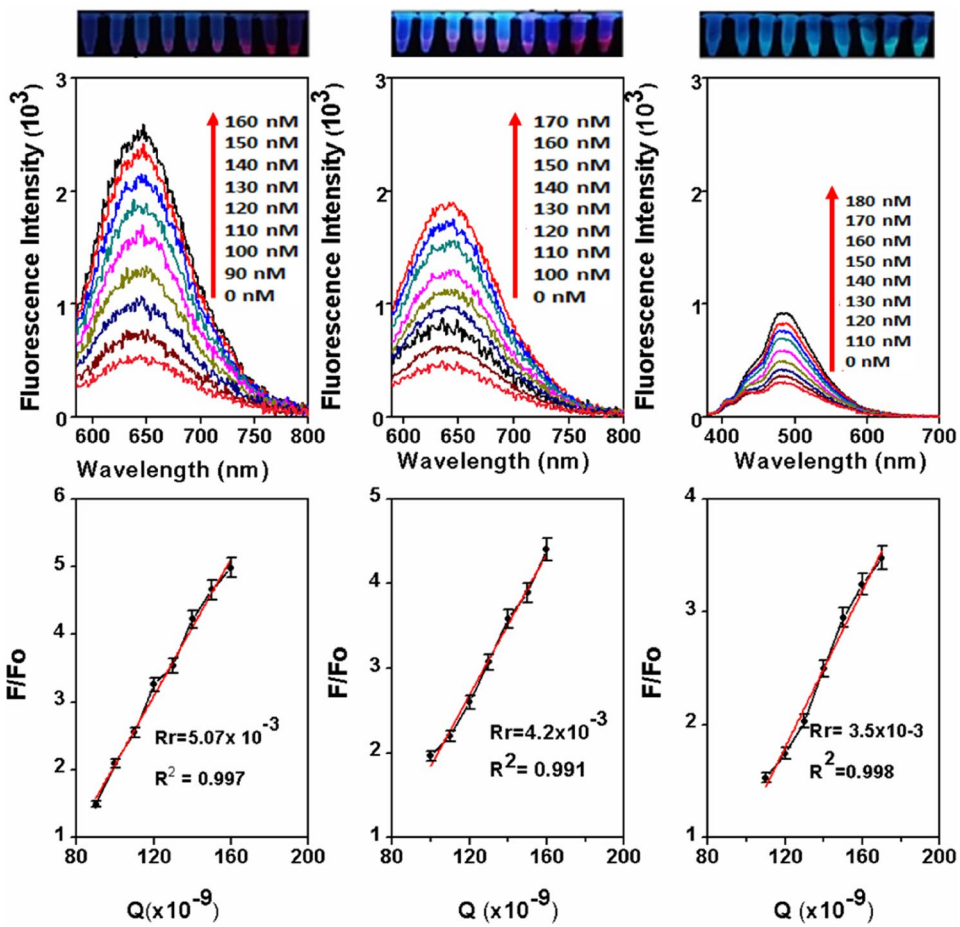

Fig. 4 MCPA induced recovery of the Cu^{2+} mediated AuNCs quenching, His-AuNCs (**a**), Lys-AuNCs (**b**) RNase-AuNCs (**c**). MCPA dependent linear relationship of relative fluorescence intensity (**d–f**)

composition of the stabilizing agent used for the respective AuNCs, different number of copper ions bind to a specific type of gold nanoclusters. For example, due to the smaller size of RNase protein (13.7 kDa) as compared to that of lysozyme (14.3 kDa), Cu^{2+} ions may effectively penetrate to interact with electron-rich groups of RNase and gold core. Conversely, more MCPA molecules can be detected on the basis of their interaction with the mineralized copper ions. For this reason, RNase-AuNCs have more pronounced fluorescence quenching and restoration response as compared to lysozyme and histidine coated gold nanoclusters. Moreover, as His-AuNCs have less quantum yield as compared to other AuNCs used in this study, therefore its sensitivity for MCPA detection is also lower than that of the other two nanoprobes. The MCPA detection limit of 90 nM (with RNase-AuNCs) is significantly lower than that of previously reported fluorescent assays for the detection of organochlorine pesticides (Discenza 2016, 2017).

The first step in this pesticide detection assay involves the binding of copper ions with Au NCs as a switch off step and second step involves selective fluorescence restoration with MCPA. In this regard, the binding efficiency of each probe with copper ions may be different. The affinity of each probe with copper ions may depend on the orientation of functional groups on each AuNC. Similarly, fluorescence restoration can be correlated with the accessibility of MCPA molecules to the copper ions bound at different points on the probe. Moreover, how efficiently these changes can be sensed by the optical probe is strongly dependent on its quantum yield. To gain further insight into the sensing mechanism of these three fluorescent probes, we determined the off–on efficiency ($E_{\text{on-off}}$) for each cluster as follows:

$$E_{\text{on}-\text{off}} = E_{\text{q}} \times E_{\text{r}},$$

while

$$E_{\text{q}} = \frac{F_{\text{o}} - F_{\text{q}}}{F_{\text{o}}},$$

and

$$E_{\text{r}} = \frac{F_{\text{r}} - F_{\text{q}}}{F_{\text{o}}},$$

where F_{o} = Fluorescence intensity in the absence of Cu, F_{q} = Fluorescence intensity in the presence of Cu, F_{r} = Fluorescence intensity when MCPA is present.

For His-AuNCs, $E_{\text{on–off}}$ value was found to be 44% while for Lys-AuNCs and RNase-AuNCs, it was found to be 47.7% and 64%, respectively. As RNase-AuNCs have comparatively higher quantum yield and due to the unsaturated gold surface, it seems more sensitive to the slight changes in its microenvironment. This data is also in accordance with the high quenching response of RNase-AuNCs when all the AuNCs were compared for the copper ions detection (Fig. S-6, A–F) in these studies.

Generally, the fluorescent methods are not much sensitive in comparison to chromatographic and mass spectrometric techniques. On the other hand, fluorescent assays are far more promising to offer rapid response, convenient and user-friendly detection methods and can also be used for high throughput assays. To compare the efficiency of our developed methods, an overview of the latest fluorescent methods developed for organochlorine pesticides is given in Table 2.

It is evident from the LOD values for organochlorine herbicides/pesticide, that our detection method is much more sensitive than most of the reported fluorescence-based nanoprobes. Moreover, as compared to quantum dots and transition metal complexes, gold nanoclusters offer a much greener approach for such analysis because of their biocompatibility and non-toxic nature.

In addition to the sensitivity, the selectivity of a detection system is also highly desired. Therefore, we evaluated the effect of -COOH (2,4-dichlorophenoxyacetic acid) and -NH_2 containing (metribuzin) pesticides during MCPA detection for the corresponding fluorescence restoration studies. The results showed negligible interference in the presence of other tested pesticides, depicting the remarkable selectivity of this detection method. Moreover, malathion, which is an organophosphorus pesticide and does not contain carboxyl or amine group, was also tested for interference studies, demonstrating negligible interference with MCPA

Table 2 A comparison of fluorescent detection methods for organochlorine pesticides

Probe	Sensing mode	LOD (nM)	References
Conjugated polymer NPs	Fluorescence turn-on detection	$\sim 5 \times 10^3$	Talbert (2016)
Europium (III) based complex	Fluorescence Decay	~4	Azab et al. (2015)
Fluorescent dye (squairaine)	Fluorescence turn on detection	$\sim 96 \times 10^3$	Tu et al. (2015)
Cadmium sulfide QDs	Fluorescence Enhancement	~150	Walia and Acharya (2014)
BIODIPY	Fluorescence Enhancement	~540	DiScenza (2017)
BIODIPY	Fluorescence Enhancement	$\sim 31 \times 10^3$	Discenza (2016)
AuNCs	Fluorescence Restoration	~9	This study

signal and thus almost 100% signal was obtained (Fig. 5). The difference in molecular weight, water solubility and varying nucleophilicity of interfering vs target molecule may be among different contributing factors for the difference of response. MCPA has the smallest molecular weight of 200.62 g/mol which is 221.04 g/mol, 214.29 g/mol and 330.358 g/mol in the case of 2,4-D, metribuzin and malathion, respectively. Substantially, MCPA has higher water solubility (825 ppm) and more nucleophilicity as compared to other interfering pesticides carrying nucleophilic oxygen, i.e., 2,4-D (677 ppm) and malathion (143 ppm). However, metribuzin is likely to show interference because of its higher water solubility (1200) but it interacts with copper via its amine group which is less electronegative in comparison to carboxylic group of 2,4-D (Gimeno 2014; Yalkowsky et al. 2016; Taghavi et al. 2016; K'Owino et al. 2018).

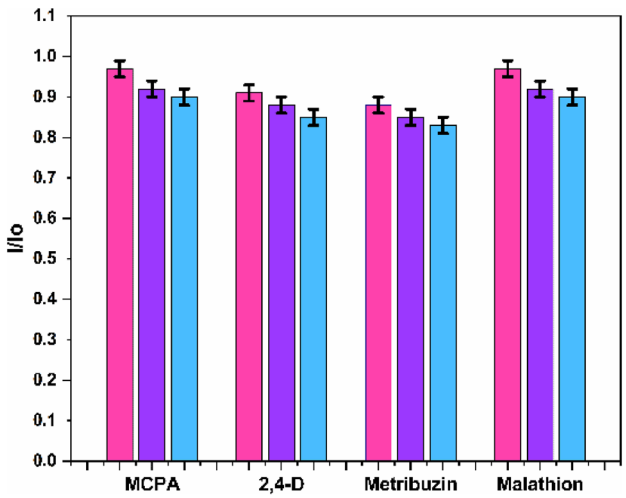

Fig. 5 The selectivity towards MCPA for RNase-AuNCs, Lys-AuNCs and His-AuNCs

As this study is being proposed for real water samples, therefore, fluorescence quenching response of all AuNCs for Cu^{2+} was checked in the presence of other potential co-existing metal ions such as Na^{1+}, K^{1+}, Ca^{2+}, Mg^{2+}, Ni^{2+}, Zn^{2+}, Pb^{2+} and Fe^{3+} present in the real water samples under the similar conditions. All these universally present ions did not show any significant interference with the histidine or lysozyme stabilized gold nanoclusters. However, the response of nickel and calcium ions showed interference with copper ions in the case of RNase-AuNCs, which may be due to the protein-Au bonding and also may be due to highly sensitive nature of RNase-AuNCs (Fig. 6a). Similarly, for restoration studies, the collateral response of different anions (PO_4^{3-}, NO_3^-, Cl^-, F, Br^-, I^-) was also examined with $-COO^-$ group but none of these anions showed interference with the response of all three types of Au nanoclusters (Fig. 6b).

We particularly selected carboxyl containing organic molecules e.g. 2,4-D. The response of all gold nanoclusters was quite selective towards MCPA even in the presence of 2,4-D (pesticide with carboxyl moiety). This selectivity might be due to the different binding ability of both pesticides with copper ions and other potential molecules. Different factors including the spatial structure, molecular weight and variation in solubility index can control the extent of this intermolecular binding (Jia 2017). This reason also explains the selectivity of our sensor in the presence of different organic molecules.

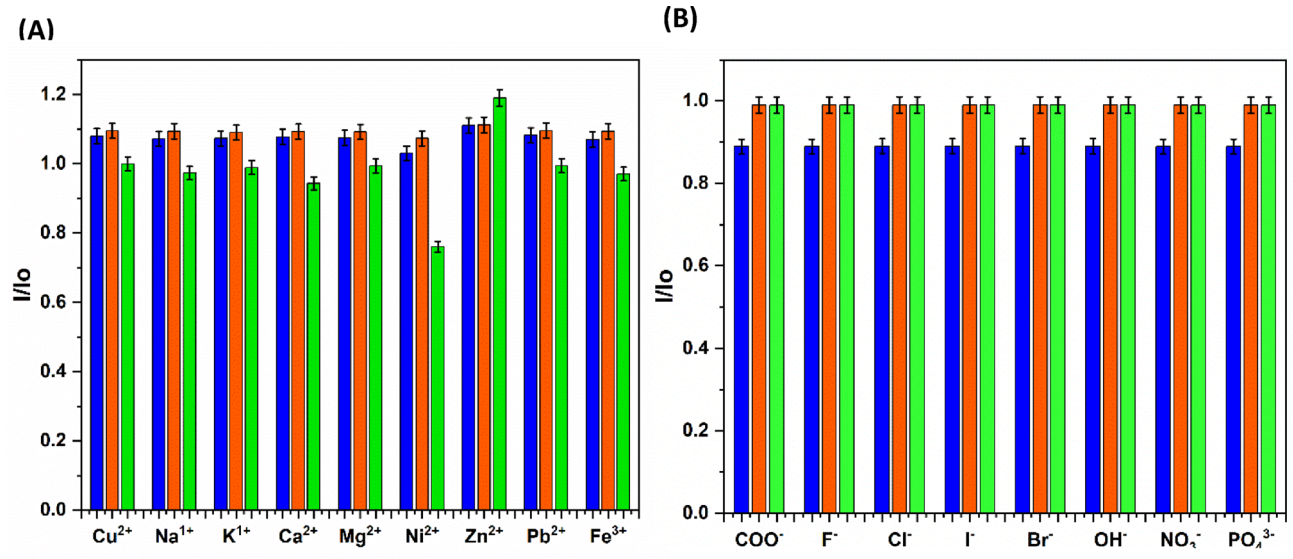

Fig. 6 The selectivity towards Cu^{2+} ions and MCPA for His-AuNCs, Lys-AuNCs and RNase-AuNCs

Optimum pH for the restoration assay was observed to be 9, 11 and 7.4 for RNase-AuNCs, Lys-AuNCs and His-AuNCs, respectively (Fig. S-7 A, B & C). The main reason behind this optimum pH trend for all three kinds of AuNCs may be due to the different isoelectric points of the proteins coated on the surface of fluorescent nanoclusters, i.e., 9.6 (Koczera 2016), 11.2 (Koirala and Banuelos 2018) and 7.59 (Dobson and Winter 2014) for RNase-A, lysozyme and histidine, respectively.

To summarize, this study demonstrates the use of fluorescent AuNCs as optical nanoprobes for the selective and sensitive determination of MCPA. This assay was validated using three different types of AuNCs as fluorescent probes. Fluorescence of all nanoclusters was quenched by Cu^{2+} while MCPA could effectively remove Cu^{2+} from the surface of fluorescent AuNCs, leading to the fluorescence recovery of all AuNCs and thus enabling the sensitive and selective detection of MCPA. The response of all three as-synthesized clusters was found to be in a linear dynamic range. The order of sensitivity for copper and MCPA was established to be as RNase-AuNCs > Lys-AuNCs > His-AuNCs. The RNase stabilized gold nanoclusters were found to be the most sensitive for MCPA detection owing to their high quantum yield. These AuNCs present ultra-sensitive detection of MCPA (up to ~ 90 nM or 18 µg/L), with detection limit much lower than the reported fluorescence-based assays for the detection of organochlorine pesticides and even below the permissible limit of 100 µg/L. These findings show that our detection method is facile, economical, sensitive and selective for the detection of MCPA and has great potential to broaden the scope of AuNCs in environmental, analytical and bioanalytical applications.

Acknowledgements Authors would like to thank National Institute of Biotechnology and Genetic Engineering, Pakistan, and the Lahore University of Management Sciences (LUMS) for providing research facilities to conduct these studies. AI wants to thank International Foundation for Science, Sweden (Grant Number W-5573) for providing funds for this work.

Author contributions All the authors in the list have solid contribution in this work.

Funding This work was supported by the funding from International Foundation for Science (Grant no: W-5573).

Data availability All the data and material included in the manuscript is available.

Compliance with ethical standards

Conflict of interest On behalf of all authors, the corresponding author states that there is no conflict of interest.

References

Abtahi S et al (2018) Size, shape, and surface coating impacts on the colloidal stability and aggregation rate of gold nanoparticles in aquatic matrices. In: Implications of shape factors on fate, uptake, and nanotoxicity of gold nanomaterials, p 118

Anirudhan TS, Alexander S (2015) Design and fabrication of molecularly imprinted polymer-based potentiometric sensor from the surface modified multiwalled carbon nanotube for the determination of lindane (γ-hexachlorocyclohexane), an organochlorine pesticide. Biosens Bioelectron 64:586–593

Azab HA, Khairy GM, Kamel RM (2015) Time-resolved fluorescence sensing of pesticides chlorpyrifos, crotoxyphos and endosulfan by the luminescent Eu(III)-8-allyl-3-carboxycoumarin probe. Spectrochim Acta Part A Mol Biomol Spectrosc 148:114–124

Carvalho FP (2017) Pesticides, environment, and food safety. Food Energy Secur 6(2):48–60

Chen J, Chen W-YYJ et al (2010) Functional gold nanoclusters as antimicrobial agents for antibiotic-resistant bacteria. Nanomedicine 5:755–764

Chen Z et al (2012) Protein-templated gold nanoclusters based sensor for off–on detection of ciprofloxacin with a high selectivity. Talanta 94(6):240–245

Damalas CA, Eleftherohorinos IG (2011) Pesticide exposure, safety issues, and risk assessment indicators. Int J Environ Res Public Health 8(5):1402–1419

Davies JED, Jabeen N (2002) The adsorption of herbicides and pesticides on clay minerals and soils. Part 1. Isoproturon. J Inclus Phenom Macrocycl C 43(3–4):329–336

Deng H-H et al (2016) Colorimetric detection of urea, urease, and urease inhibitor based on the peroxidase-like activity of gold nanoparticles. Anal Chim Acta 915:74–80

Dias AN et al (2015) Use of green coating (cork) in solid-phase microextraction for the determination of organochlorine pesticides in water by gas chromatography-electron captu. Talanta 134:409–414

Discenza D (2016) Supporting parents with mental health support in the NICU. NN 35(1):42–44

DiScenza DJ et al (2017) Detection of organochlorine pesticides in contaminated marine environments via cyclodextrin-promoted fluorescence modulation. ACS Omega 2(12):8591–8599

Dobson CM, Winter NS (2014) The identification of amino acids by interpretation of titration curves: an undergraduate experiment for biochemistry. World J Chem Educ 2(4):59–61

Durgadas CV, Sharma CP, Sreenivasan K (2011) Fluorescent gold clusters as nanosensors for copper ions in live cells. Analyst 136(5):933–940

Eto M (2018) Organophosphorus pesticides. CRC, Oxford

Gao L, Ju L, Cui H (2017) Chemiluminescent and fluorescent dual-signal graphene quantum dots and their application in pesticide sensing arrays. J Mater Chem C 5(31):7753–7758

Gimeno O et al (2014) Ozonation of 4-chloro-2-methylphenoxyacetic acid (MCPA) in an activated sludge system. J Chem Technol Biotechnol 89(8):1219–1227

Goswami N et al (2016) Luminescent metal nanoclusters with aggregation-induced emission. J Phys Chem Lett 7(6):962–975

Heys KA et al (2017) Levels of organochlorine pesticides are associated with amyloid aggregation in apex avian brains. Environ Sci Technol 51(15):8672–8681

Ibrahim IA, Abbas AM, Darwish HM (2017) Fluorescence sensing of dichlorvos pesticide by the luminescent Tb (III)-3-ally-salicylohydrazide probe. Luminescence 32(8):1541–1546

Jayaraj R, Megha P, Sreedev P (2016) Organochlorine pesticides, their toxic effects on living organisms and their fate in the environment. Interdiscip Toxicol 9(3–4):90–100

Jia M et al (2017) A molecular imprinting fluorescence sensor based on quantum dots and a mesoporous structure for selective and sensitive detection of 2, 4-dichlorophenoxyacetic acid. Sens Actuators B Chem 1(252):934–943

Jiang D et al (2016) Fluorescent switch sensor for detection of anticancer drug and ctDNA based on the glutathione stabilized gold nanoclusters. Sens Chem 232:276–282

K'Owino IO, Masika K, Okello VA (2018) Kinetics of degradation of metribuzin in aqueous solution using zero valent iron nanoparticles. Al-Nahrain J Sci 21(2):1–9

Kah M et al (2007) Behaviour of ionisable pesticides in soils. PhD Thesis

Kalwar A, Jamali NH et al (2015) Catalytic degradation of imidacloprid using L-serine capped nickel nanoparticles. Mater Express. 5(2 SRC-BaiduScholar):121–128

Katagi T (2010) Bioconcentration, bioaccumulation, and metabolism of pesticides in aquatic organisms, reviews of environmental contamination and toxicology, Springer. 2010 SRC—BaiduScholar, pp 1–132

Koczera P et al (2016) The ribonuclease a superfamily in humans: canonical RNases as the buttress of innate immunity. Int J Mol Sci 17(8):1278

Koirala P, Banuelos JL (2018) The inverse and direct Hofmeister series of Hen egg lysozyme at pH below isoelectric point (pI) as seen by SAXS. Bull Am Phys Soc 106(36):15249–15253

Kong Y et al (2013) Near-infrared fluorescent ribonuclease-A-encapsulated gold nanoclusters: preparation, characterization, cancer targeting and imaging. Nanoscale 5(3):1009–1017

Kumar P, Kim KH, Deep A (2015) Recent advancements in sensing techniques based on functional materials for organophosphate pesticides. Biosens Bioelectron 70:469–481

Lai X et al (2017) Coordination-induced decomposition of luminescent gold nanoparticles: sensitive detection of H_2O and glucose. Anal Bioanal Chem 409(6):1635–1641

Le Guével X et al (2011) NIR-emitting fluorescent gold nanoclusters doped in silica nanoparticles. J Mater Chem 21(9):2974–2981

Li J, Zhu K, Xu JJ (2014) Fluorescent metal nanoclusters: from synthesis to applications. Tr Anal Chem. 58(SRC-BaiduScholar):90–98

Li X et al (2018) Development and application of a novel fluorescent nanosensor based on FeSe quantum dots embedded silica molecularly imprinted polymer for the rapid optosensing of cyfluthrin. Biosens Bioelectron 99:268–273

Lin C-AJ et al (2009) Synthesis, characterization, and bioconjugation of fluorescent gold nanoclusters toward biological labeling applications. ACS Nano 3(2):395–401

Lu H, Quan S, Xu S (2017) Highly sensitive ratiometric fluorescent sensor for trinitrotoluene based on the inner filter effect between gold nanoparticles and fluorescent nanoparticles. J Agric Food Chem 65(44):9807–9814

Luo J et al (2016) Fluorescent turn-on determination of the activity of peptidases using peptide templated gold nanoclusters. Microchim Acta 183(2):605–610

Markechová AD, Tomková M, Sádecká J (2013) Fluorescence excitation-emission matrix spectroscopy and parallel factor analysis in drinking water treatment. Pol J Environ Stud 22(5):1289–1295

Oh E et al (2016) Energy transfer sensitization of luminescent gold nanoclusters: more than just the classical förster mechanism. Sci Rep 6:35538

Ramesh BS et al (2016) Detection of cell surface calreticulin as a potential cancer biomarker using near-infrared emitting gold nanoclusters. Nanotechnology 27(28):285101

Shamsipur M et al (2015) Novel blue-emitting gold nanoclusters confined in human hemoglobin, and their use as fluorescent probes for copper (II) and histidine. Microchim Acta 182(5–6):1131–1141

Skiba E, Kobyłecka J, Wolf WM (2017) Influence of 2,4-D and MCPA herbicides on uptake and translocation of heavy metals in wheat (*Triticumaestivum* L.). Environ Pollut (Barking, Essex: 1987) 220(Pt B):882–890

Taghavi S et al (2016) Microbial compositions for use in combination with soil insecticides for benefiting plant growth. United States patent application US 14/870, p 349

Talbert W et al (2016) Turn-on detection of pesticides via reversible fluorescence enhancement of conjugated polymer nanoparticles and thin films. N J Chem 40:7273–7277

Tao Y et al (2015) Metal nanoclusters: novel probes for diagnostic and therapeutic applications. Chem Soc Rev 44(23):8636–8663

Tsoi KM et al (2013) Are quantum dots toxic? Exploring the discrepancy between cell culture and animal studies. Acc Chem Res 46(3):662–671

Tu L, Xu J et al (2015) Near-infrared fluorescent turn-on detection of paraquat using an assembly of squaraine and surfactants. Sens Chem 215(SRC BaiduScholar):382–387

Walia S, Acharya A (2014) Fluorescent cadmium sulfide nanoparticles for selective and sensitive detection of toxic pesticides in aqueous medium. J Nanopart Res 16(12):1–10

Walton I et al (2012) A fluorescent dipyrrinone oxime for the detection of pesticides and other organophosphates. Organ Lett 14(11):2686–2689

Wang Y et al (2013) Functionalized quantum dots for biosensing and bioimaging and concerns on toxicity. ACS Appl Mater Interfaces 5(8):2786–2799

Wang C et al (2015) A phosphole oxide based fluorescent dye with exceptional resistance to photobleaching: a practical tool for continuous imaging in STED microscopy. Angew Chem (International ed. in English) 54(50):15213–15217

Yalkowsky SH, He Y, Jain P (2016) Handbook of aqueous solubility data. CRC, Boca Raton

Yan X et al (2017) A novel fluorimetric sensing platform for highly sensitive detection of organophosphorus pesticides by using egg white-encapsulated gold nanoclusters. Biosens Bioelectron 91:232–237

Yang X et al (2011) Blending of HAuCl 4 and histidine in aqueous solution: a simple approach to the Au 10 cluster. Nanoscale 3(6):2596–2601

Zhang S, Zhang R-LSQ et al (2017) Simple and sensitive fluorescence assay for acetylcholinesterase activity detection and inhibitor screening based on glutathione-capped gold nanoclusters. Sens Chem 253:196–202

Zhao X et al (2017) Development strategies and prospects of nano-based smart pesticide formulation. J Agric Food Chem 66(26):6504–6512

Zheng Q et al (2014) Ultra-stable organic fluorophores for single-molecule research. Chem Soc Rev 43(4):1044–1056

Zhou W et al (2016) Ultrastable BSA-capped gold nanoclusters with a polymer-like shielding layer against reactive oxygen species in living cells. Nanoscale 8(18):9614–9620